Research Square

Preprints are preliminary reports that have not undergone peer review.
They should not be considered conclusive, used to inform clinical practice,
or referenced by the media as validated information.

Evaluating the Mosquito Weather Index: A simple tool for predicting and communicating mosquito activity

Antonios Michaelakis
Benaki Phytopathological Institute
Georgios Balatsos
Benaki Phytopathological Institute
Vasileios Karras
Benaki Phytopathological Institute
Dimitrios Papachristos
Benaki Phytopathological Institute
Rachel Lowe
Barcelona Supercomputing Center
Frederic Bartumeus
Centre d'Estudis Avançats de Blanes
Ioannis Lemesios
National Observatory of Athens
Christos Giannakopoulos
National Observatory of Athens
Konstantinos Lagouvardos
National Observatory of Athens
John Palmer
john.palmer@upf.edu

Universitat Pompeu Fabra

Article

Keywords:

Posted Date: September 9th, 2026

DOI: https://doi.org/10.21203/rs.3.rs-10821362/v1

License: This work is licensed under a Creative Commons Attribution 4.0 International License.
Read Full License

Additional Declarations: No competing interests reported.

Evaluating the Mosquito Weather Index: A simple tool for predicting and communicating mosquito activity

Antonios Michaelakis[1], Georgios Balatsos[1], Vasileios Karras[1], Dimitrios Papachristos[1], Rachel Lowe[2, 3, 4], Frederic Bartumeus[3, 5, 6], Ioannis Lemesios[7], Christos Giannakopoulos[7], Konstantinos Lagouvardos[7], and John R.B. Palmer[8,*]

[1]Scientific Directorate of Entomology and Agricultural Zoology, Benaki Phytopathological Institute, Delta Str. 8, 14561, Kifissia, Attiki, Greece
[2]Centre on Climate Change & Planetary Health & Centre for Mathematical Modelling of Infectious Diseases, London School of Hygiene & Tropical Medicine (LSHTM), London, United Kingdom
[3]Institució Catalana de Recerca i Estudis Avançats, ICREA, Barcelona, Spain
[4]Barcelona Supercomputing Center (BSC), Barcelona Spain
[5]CREAF, Cerdanyola del Vallès, Spain
[6]Department of Ecology and Complexity, Centre d'Estudis Avançats de Blanes (CEAB-CSIC), Girona, Spain
[7]Institute of Environmental Research and Sustainable Development, National Observatory of Athens, I. Metaxa & Vas. Pavlou, GR-15236 Palea Penteli, Greece
[8]Department of Politics and Social Sciences, Universitat Pompeu Fabra, Barcelona, Spain
[*]john.palmer@upf.edu

ABSTRACT

The Mosquito Weather Index (MWI) is the first operational index to translate the combined effects of temperature, humidity and wind speed into a single measure of mosquito activity, communicated to the public and public-health stakeholders in an easy-to-act-on form. The index ranges from 0 to 1 and maps to five activity levels, from "no activity" to "very high activity." This study presents the first empirical evaluation of the MWI. We assess its predictions of vector mosquito counts from adult suction traps in Moschato-Tavros, Attica, Greece, during 2018 and 2019. We find the MWI is strongly associated with *Aedes albopictus* and *Culex pipiens* trap counts. The single MWI variable improves predictions of trap counts—both in cross-validation and in forward forecasts—from models that lack information on weather or seasonality, while adding little once such information is included. We also evaluate different methods, finding that temporally fine-grained (hourly) weather data is crucial for its performance. These findings suggest that the MWI functions as intended, offering a simple, interpretable predictor of vector mosquito activity that can be acted on by the general public and mosquito-control specialists.

Introduction

Mosquito-borne diseases represent a growing public health concern globally, and climate and weather conditions play a pivotal role in shaping mosquito activity and transmission dynamics[1]. In Greece, West Nile virus (WNV) has become a persistent threat, with the first major outbreak recorded in 2010[2,3]. Since then, seasonal outbreaks have occurred regularly, generally during summer and early autumn, when mosquito populations peak, although their timing varies: the 2018 season, the first of our study period, began unusually early across Europe[4]. The virus is primarily transmitted by *Culex pipiens* mosquitoes, with birds serving as reservoir hosts[2]. The geographical distribution of WNV in Greece has expanded over time, with cases reported in both rural and urban areas, including the Attica Region[5,6], home to around 3.8 million people, more than 36% of the country's population[7]. Several factors have been associated with the increasing risk of WNV transmission, including climate change, urbanisation, and land-use alterations[5,8].

In parallel, the invasive mosquito species *Aedes albopictus* has become established in Greece after having been first detected in 2003–2004[9]. It is an aggressive daytime biter that proliferates in urban environments and serves as a vector for numerous arboviruses, including dengue, chikungunya, and Zika[10,11]. The species has expanded its range in Greece, especially in urban and suburban areas, where it exploits artificial water containers for reproduction, making its management difficult[11–13]. This vector has been found to spread in cars[14,15] and to remain active even during the winter months in the Attica Region, substantially increasing the challenges and efforts required for public health protection[16].

The need for models and tools to predict vector-borne diseases and the dynamics of mosquito vectors has become increasingly critical in the face of these developments. Models can provide essential insights into the spatial and temporal

distribution of vector mosquito populations and the risk of disease transmission, enabling timely interventions to mitigate outbreaks[17–21]. Making models useful for guiding mosquito control operations or enabling communities to avoid risks often requires innovative tools that can translate complex relationships into simple, clear guidance[22].

The Mosquito Weather Index (MWI) is one such tool. Developed through a collaboration between the Benaki Phytopathological Institute and the National Observatory of Athens under the LIFE CONOPS project (LIFE12 ENV/GR/000466), this index draws on thermo-biological insights to capture non-linear relationships between mosquito activity and key weather variables. Combining temperature, relative humidity, and wind speed, the MWI generates simple, clear alerts in five categories, ranging from "no activity" to "very high activity." Since its integration into the Greek weather forecast platform (`https://meteo.gr`) in June 2014, the MWI has provided real-time predictions to the public, aiding in mosquito awareness and control efforts. Despite its widespread application and potential, the MWI's predictive accuracy has not been previously tested. Nor has there been rigorous exploration of the different weather-data sources from which it can be constructed, or of its potential to improve statistical models of mosquito abundance by offering a more parsimonious, biologically grounded way of incorporating weather information.

This study fills those gaps, testing the relationship between MWI and the counts of adult mosquitoes captured in traditional suction traps, evaluating the MWI's predictive accuracy and assessing how the MWI's performance depends on modellers' choices of weather data sources and approaches to integrating weather values over time. We rely on a total of 360 collections from six BG-Sentinel 2 traps (Biogents AG, Regensburg, Germany), baited with BG-Lure cartridges, in Attica, Greece, between July 2018 and October 2019 to validate the predictive performance of the MWI.

Results

The results show a high correlation between MWI and traditional trapping outcomes, and they show that MWI improves the predictive accuracy of traditional trap count models. They also show that this depends on how models are specified, which sources of weather data are chosen, and how the index is calculated. We focus our analysis on a set of zero-inflated negative binomial multilevel regression models controlling for trapping effort (days elapsed between when trap was set and when it was checked) and trap random effects, with the MWI calculated hourly from weather variables, aggregated by day using the maximum MWI value for each 24-hour period, and then averaged over each trapping period. We compare results across models with and without a seasonality term (a function of day-of-year), and across a variety of alternative specifications, including models with MWI aggregate by day using means instead of maximums, and using only daylight hours (which we term daylight time, DT) or only the two hours after sunrise together with the two hours before sunset (which we term activity time, AT, based roughly on peak *Ae. albopictus* and *Cx. pipiens* activity[23]). Finally, we explore the performance of MWI calculated from different weather data sources.

Association with trap counts

We find that the MWI is strongly associated with *Aedes albopictus* and *Culex pipiens* trap counts. When modelled with the zero-inflated negative binomial multilevel regression, the coefficient on MWI for both species is credibly positive in the count component of the model and credibly negative in the zero-inflation component (Figure 1b and Supplementary Table S4). In other words, increases in MWI are associated with higher trap counts and with lower probabilities of structural zeros (i.e. no mosquitoes in the trap). Figure 1a shows the resulting relationship between MWI and expected trap counts for each species. The full posterior distributions of all model coefficients are provided in Supplementary Figures S3 and S4.

This result is robust across a variety of model specifications. Figure 2 summarises the index coefficient across alternate models, including (a) Poisson models and negative binomial models without a zero-inflation term, (b) the inclusion of a seasonality term in the models, and (c) different approaches to aggregating MWI. When seasonality is not included, most models have positive coefficients on MWI for the count component and negative coefficients on it for the zero-inflation component. Results are more mixed once seasonality is added to the model. Supplementary Figure S6 includes comparisons across additional specifications.

Predictive accuracy

In addition to its association with trap counts, the single MWI variable clearly improves the predictive accuracy of the trap models.[1] This improvement can be seen from leave-one-out cross validation: adding MWI to a model that includes only trapping effort (the amount of time for which each trap was set) and trap random effects (see Methods section) substantially raises the expected log predictive density (ELPD) for both species (Supplementary Fig. S5). At the same time, MWI does not offer clear improvements to trap count models that have already been trained on a term that captures seasonality. Once

[1]We use predictive accuracy here as an umbrella term for out-of-sample predictive performance, encompassing perfomance estimated by leave-one-out cross-validation as well as forecasting skill estimated by leave-future-out validation—in which models are refit at each time step using only past data.

day-of-year is in the model, MWI appears redundant for the relatively short time period under study. (As discussed further below, this redundancy may not hold for longer time periods.)

This pattern largely holds across the set of alternate model specifications. Figure 3 shows the leave-one-out predictive gain of each MWI model relative to its matched no-MWI version: in the pairs that do not include a seasonality term, the MWI models show large gains over their no-MWI versions, while in the pairs that include the seasonality term the differences are close to zero for *Ae. albopictus*. They do not vanish entirely for *Cx. pipiens* or for the pooled total, however: under maximum aggregation, adding MWI to a seasonal model still improves held-out prediction by roughly 12–17 ELPD units for *Cx. pipiens* in the negative binomial models and 21–36 for the pooled total, with 90% intervals excluding zero. The Supplementary Information includes comparisons across additional model specifications (Supplementary Fig. S7).

The same pattern holds when models instead account for weather directly rather than through MWI. Under the primary specification, models containing only the single MWI value predict trap counts about as well as one containing the three raw weather variables—relative humidity, temperature and wind speed—entered linearly, and only modestly worse than one entering them as second-degree polynomials; all three greatly exceed the trapping-effort-only null (Supplementary Table S5). MWI thus behaves as a parsimonious, one-parameter summary of the weather variables, recovering most of their count-relevant predictive information, so that models already containing that weather information have little further to gain from MWI.

We also find that MWI improves forecasting skill for models that do not include a seasonality term. Figure 4 shows ΔELPD gain from adding MWI to models that otherwise include only trapping effort and trap random effects, based on leave-future-out cross validation. This calculation is done by training models, at each time step, only on past trap count data and then forecasting the next month using MWI calculated from that month's observed weather. In other words, we ignore the uncertainty of weather predictions here, and focus only on the impact of MWI. Across most forecast months MWI raises the forward ΔELPD for both species. Consistent with the leave-one-out results, once a seasonal trend is included, the additional forecasting value of MWI is small: slightly negative on balance for *Ae. albopictus* and small but positive for *Cx. pipiens*, concentrated in the warm season (Figure 5).

This leave-future-out pattern is stable across the same grid of model specifications used above (Supplementary Fig. S8), which shows the pooled forward ΔELPD of each MWI model relative to its matched no-MWI version across daily aggregation window, aggregation statistic, distribution family, and whether a seasonal term is present. Without seasonality the negative-binomial and zero-inflated negative-binomial models show consistent forecasting gains from MWI; once a seasonal term is added the gains shrink toward zero, mirroring the leave-one-out results.

Weather measurement and aggregation

Whereas our results are largely robust across model specifications, they are sensitive to the choice of weather data used to calculate MWI and to the way in which calculations are made. All results, thus far, are based on MWI calculated from hourly weather data from the Copernicus Climate Change Service (ERA5-Land hourly). MWI is calculated hourly and then aggregated by day using the maximum or mean value across each full 24-hour period. Leave-one-out cross validation shows that aggregation using maximum MWI values generally performs better than aggregation using means. Daily aggregation can also be done using only weather values from periods of daylight (DT) or from the two-hour periods after sunrise and before sunset (AT), when *Ae. albopictus* is known to be most active[23]. Restricting aggregation to these windows, however, does not systematically improve on the full 24-hour summary. In our leave-one-out comparisons, the best performing window depends on the statistic it is paired with. Under maximum aggregation the daylight window is marginally the best of the three for all three outcomes, though its margin over the full day is credible only for *Cx. pipiens*, whereas the narrower post-sunrise/pre-sunset window (AT) does somewhat worse for *Ae. albopictus* and the pooled total, and about the same for *Cx. pipiens*. Under mean aggregation that ordering reverses and the daylight window becomes the worst of the three, in some cases by a wide margin (Figure 3). Of the two choices the aggregation statistic is the more consistent: maximum-based aggregation outperforms mean-based aggregation in every one of the 18 non-seasonal negative-binomial and zero-inflated negative-binomial specifications, and by more than twice the standard error of the paired difference in 15 of them, whereas no window is best regardless of the statistic used with it.

Importantly, however, in all of the choices discussed so far, MWI is calculated based on hourly weather data and then aggregated by day. Because MWI is a non-linear function of three weather variables, aggregating weather by day first and then calculating MWI using daily means, maximums, or minimums of each weather variable produces very different results—and we find that MWI calculated in this way is largely uncorrelated with trap counts. Calculating MWI from any weather dataset that has already been aggregated by day produces the same results. We find this when we fit the primary specification using MWI calculated from the daily maxima of each weather variable in the Athens weather station series from the Hellenic Data Service (Helix-daily). The count-component coefficient on MWI, credibly positive when the index is computed hourly from ERA5-Land, becomes indistinguishable from zero for *Ae. albopictus* (0.24, 90% CrI −0.42 to 0.91) and for the pooled total, and credibly *negative* for *Cx. pipiens* (−0.88, −1.49 to −0.27); leave-one-out accuracy falls by 37 to 65 ELPD units relative to the hourly-computed index (Supplementary Table S8). Over the same trapping periods the correlation between index and trap

counts drops from 0.26 to 0.05 for *Ae. albopictus* and from 0.25 to −0.04 for *Cx. pipiens*. The daily index does retain some capacity to flag periods with no catch at all—its zero-inflation coefficient remains strongly negative—so it still improves on a weather-free null, substantially so for *Ae. albopictus*; but as a predictor of abundance it fails. Any weather dataset distributed only at daily resolution is subject to the same limitation.

A potential improvement over gridded reanalysis products such as ERA5-Land hourly could be the use of high-quality in situ meteorological observations collected near trapping locations. We tested this using HOBO temperature and relative-humidity loggers installed at four of the six BG traps. Three features of these data limit their usefulness here. First, the loggers do not record wind speed, so an MWI computed from them must borrow its wind term from another source. Second, coverage is incomplete: only four of the six traps carried a logger, and even at those traps about 4% of the expected 30-minute relative humidity readings are either missing or were discarded because they showed implausible values (Supplementary Table S3). Third, and most consequentially, the logger relative humidity readings run systematically drier than those from the ERA5-Land hourly data: hour by hour they are about 4 percentage points (roughly 5%) lower than the ERA5 values on average. Because the MWI is a non-linear function of humidity that drops to zero below 40% relative humidity, the impact of the lower HOBO relative humidity is amplified when this is converted to MWI: substituting the logger relative humidity for the ERA5-Land hourly relative humidity forces the MWI to zero in about 10% of the hours for which it is positive when computed from ERA5 (Supplementary Figures S1 and S2). Consequently, an MWI built from the on-site loggers is a poorer predictor of trap counts than one built from ERA5-Land. In a leave-one-out comparison restricted to the trap-periods with logger coverage, substituting the HOBO MWI for the ERA5 MWI lowered the expected log predictive density for both species (by about 57 for *Ae. albopictus* and 21 for *Cx. pipiens*, with standard errors of the difference of 9 and 8, respectively; Supplementary Table S6); the HOBO-based MWI improved only modestly on a trapping-effort-only model for *Ae. albopictus* and negligibly for *Cx. pipiens*, whereas the ERA5-based MWI improved on it substantially for both species. The same shift is visible in the fitted coefficients: the credibly positive count-component coefficient on MWI obtained with the ERA5-Land hourly data drops to approximately zero when MWI is instead computed from the HOBO readings.

Discussion

Our results show the Mosquito Weather Index performing in ways that are consistent with its intended function. The index is strongly and credibly associated with the number of female *Ae. albopictus* and *Cx. pipiens* caught in BG-Sentinel traps: Higher MWI values predict larger counts and lower probability of an empty trap, and this holds across model specifications, aggregation windows, and aggregation statistics. Moreover, the single MWI variable improves the predictive accuracy, including forecasting skill, of models that lack information on weather or seasonality, and it does so about as well as adding the three underlying weather variables directly, whether as linear terms or as second-degree polynomials. Although the MWI adds little to models that already include weather or seasonality terms, redundancy in a fitted model need not imply redundancy in operational use: a day-of-year term captures only the average seasonal cycle over the study period, whereas the MWI tracks the weather that actually occurs, distinguishing a given week from the same week in a typical year. Over periods longer than our two trapping seasons, and under year-to-year variability or a changing climate, we would expect this distinction to grow in importance. The value of the MWI lies in its simplicity, as a parsimonious way to predict vector mosquito activity. Furthermore, this single index is straightforward and understandable to the general public as well as to mosquito control decision-makers.

Our results also provide valuable insights into the best data and methods for constructing MWI. We found that the index performed well when constructed from ERA5-Land hourly data. We had expected it to perform even better when constructed from HOBO-30min data, given that this data captures conditions closer to the mosquitoes themselves, but we found the opposite: Although the HOBO weather variables performed well when modelled directly, MWI had lower predictive accuracy when calculated from HOBO temperature and humidity readings (Supplementary Table S9), which also bounds what the thresholds cost: a single MWI value recovers most of the predictive gain available from flexible functions of the same three variables (Supplementary Table S5), so modifying the breakpoints could improve on it only modestly. This suggests that the MWI is not calibrated to the type of microclimate data the HOBO sensors measure, but such calibration could be done in a future study. We note too that our weekly trap-collection interval (the loggers themselves record every 30 minutes) may wash out some of the fine-scale variation these sensors are best placed to capture.

Most importantly, we found that calculating MWI from aggregated weather data does not work well: As a non-linear function of three weather variables, MWI calculated from daily means, minima or maxima of these variables is very different from MWI calculated from hourly weather readings and *then* aggregated, and the latter approach is the only one that consistently performed well in our analysis. This is, again, consistent with the way MWI was designed, as a real-time tool for predicting and communicating mosquito activity based on current weather conditions.

To the extent that MWI needs to be aggregated, we found that daily maximums consistently outperformed daily means in our BG trap models. It appears that trap catches respond to whether a day contained a window of favourable conditions more than to how favourable the day was on average. The choice of hours used in the aggregation also matters, but less so and in

more complicated ways: restricting attention to the hours around sunrise and sunset, when *Ae. albopictus* is most active, did not improve *Ae. albopictus* prediction and made little difference for *Cx. pipiens*. For operational purposes, simply using the daily maximum over the full 24 hours appears to be the most reliable approach.

All of this matters because ongoing ecological and epidemiological shifts are heightening the need for effective surveillance and control strategies to mitigate vector-borne disease outbreaks. In Greece, *Cx. pipiens* can maintain WNV circulation through the winter, so overwintering populations may contribute to the re-establishment of transmission in the following season[24]; USUV has likewise been detected in Greek *Cx. pipiens*[25]; and WNV activity during the summer of 2026 reached notable levels compared with previous years[26]. This highlights the importance of year-round rather than summer-only surveillance.

Moreover, weather-based forecasting is emerging as an essential tool for early warning and for facilitating evidence-based vector control and exposure reduction strategies[27]. Given how strongly mosquito ecology is influenced by temperature, humidity, and other environmental conditions[28], the integration of meteorological variables with reliable mosquito surveillance data can improve forecasting models and provide estimates of both mosquito abundance and disease risk, allowing public health authorities to optimise surveillance, implement timely mosquito control measures and communicate preventive actions before typical transmission periods. Weather-driven forecasting models can reliably predict mosquito abundance several weeks in advance[29,30], and incorporating microclimatic conditions into these models has been reported to substantially improve predictions of mosquito population dynamics, as breeding and resting sites often experience temperatures that differ markedly from ambient weather station measurements[31]. More broadly, models of climate-driven changes in mosquito phenology, development rates and population dynamics are providing actionable forecasts across spatial and temporal scales and highlighting the importance of locally validated predictive tools[32].

Integrating meteorological variables into mosquito population models, however, is complicated due to the non-linear effects of multiple weather variables at once. The MWI offers a simple and operationally feasible alternative: to our knowledge, it is the first operational index to translate the combined effects of temperature, humidity and wind speed into a simple, interpretable metric of mosquito activity. Having validated and tested its predictive accuracy here, we show that it can serve directly as a forecasting index—requiring no ongoing recalibration—for public health professionals and the general public alike, thereby facilitating risk communication and decision-making.

The MWI is a valuable advancement in mosquito surveillance and control, providing a practical tool for predicting mosquito activity based on weather conditions. Its application in the municipality of Moschato-Tavros (Greece) demonstrates its potential for guiding targeted interventions, particularly in urban and semi-urban settings where mosquito-driven arbovirus circulation is an increasing concern[16,24,25]. Evidence-based interventions are a cornerstone of integrated vector management (IVM)[33], and MWI forecasts can serve as a useful tool to enhance resource allocation efficiency, optimising climate-driven larviciding and adulticiding applications[34], and to improve the accuracy of control actions[35]. In addition, public awareness is a key component of effective IVM programmes[36,37]. Over the past 12 years, the MWI has functioned as intended, providing a simple and interpretable predictor of mosquito vector activity that integrates the complex effects of weather into a single operational metric. This helps risk communication and enables the general public to better understand periods of increased mosquito activity, promoting contextually informed self-protection behaviors. Moreover, the MWI is a valuable decision-support tool for mosquito control specialists, offering relevant information on weather conditions conducive to enhanced surveillance and targeted vector control operations.

Despite these promising outcomes, the current study has limitations. The BG trap datasets were based on weekly sampling intervals and not on 24-hour trapping data, which may have limited the temporal resolution of mosquito abundance estimates and potentially influenced the interpretation of short-term variations in vector activity. More frequent or continuous sampling could provide a more detailed understanding of mosquito population dynamics. Additionally, the study's focus on a single municipality in Attica could limit the generalisability of findings to regions with different ecological and climatic conditions.

Future research should aim to validate the index across diverse geographical settings and incorporate additional environmental factors, such as precipitation and land use, to enhance its predictive accuracy[38–40]. A promising research direction is exploring the relationship between the MWI and the basic reproduction number (R_0) of mosquito-borne diseases, such as dengue. By studying the relationship between MWI and the seasonal distribution and abundance of *Ae. albopictus*, researchers could develop models to predict disease transmission dynamics and identify high-risk periods for outbreaks. This approach would not only refine the MWI's utility but also provide crucial insights for designing more effective public health interventions[41,42]. Further, the MWI could be extended to provide early warnings of mosquito activity using subseasonal to seasonal forecasts of weather variables, to provide lead times from several weeks to several months in advance[43,44].

Public awareness and engagement are essential components of integrated mosquito management, as individual actions can significantly influence the availability of mosquito breeding habitats and the effectiveness of control programs. Innovative communication tools that combine scientific information with real-time, easily accessible guidance can play a key role in promoting community participation. In Greece, the MWI, publicly available since 2014 through the Greek weather forecasting platform (https://meteo.gr) represents such an approach. Taking advantage of a highly visited national weather

information platform, the index provides daily estimates of mosquito activity levels while simultaneously delivering practical recommendations to citizens on how to reduce mosquito breeding sites and adopt effective personal protection measures. Beyond its role as a public information and risk communication tool, the platform has also supported research activities by enabling the implementation of a nationwide web-based questionnaire designed to investigate the impact and public perception of invasive mosquito species in Greece[36]. The survey aimed to assess citizens' awareness of the *Ae. albopictus* problem, their perceptions of mosquito-related risks, the economic burden associated with personal prevention measures and their preferences regarding mosquito control strategies and policy priorities within a changing socio-ecological context. The possible integration of digital tools, such as the MWI and citizen science approaches like the Mosquito Alert mobile application (implemented in Greece at `https://mosquitoalert.conops.gr`, and worldwide at `https://mosquitoalert.com`), provides complementary opportunities for public engagement and mosquito surveillance. While the MWI supports risk communication and awareness by providing timely information on mosquito activity and prevention measures, Mosquito Alert enables citizens to actively contribute observations on mosquito presence and distribution[45–47]. Together, these platforms enhance public participation, improve data availability, and support evidence-based integrated mosquito management strategies.

Methods

Study area

The study was carried out in the municipality of Moschato-Tavros (MT), situated in the South Athens Regional Unit of the Attica Region, and encompassing the southwestern part of the Athens urban area. The municipality comprises two primary districts: Moschato and Tavros. Geographically, it is located at approximately 37°57′N latitude and 23°41′E longitude, covering a total area of 4.45 km^2. According to the 2021 census, the population stands at 39,661 inhabitants[7]. Moschato-Tavros serves as a valuable study area due to its diverse land use patterns, including urban, semi-urban, and green spaces, which influence mosquito breeding and activity.

Mosquito trap data

Adult mosquitoes were sampled using BG-Sentinel 2 traps (Biogents AG, Regensburg, Germany) baited with BG-Lure cartridges, following the European Centre for Disease Prevention and Control guidelines for the surveillance of native and invasive mosquitoes in Europe[48]. Six traps were deployed across the study area—three in the Moschato district and three in Tavros—and serviced on a weekly basis; their locations are shown in Figure 6. After each collection the trap nets were transported under refrigerated conditions to the Laboratory of Insects and Parasites of Medical Importance at the Benaki Phytopathological Institute and held at $-20\,^{\circ}$C to ensure mortality. Specimens were then identified according to species under a stereomicroscope using validated morphological keys[49,50]. At each collection we recorded the number of female *Aedes albopictus* and *Culex pipiens* captured, together with the trapping period, defined as the number of days the trap had been running since the previous servicing. This trapping period is retained in the analysis as a measure of sampling effort (see *Statistical analysis*).

Trap data was processed for statistical analysis by loading from the source workbooks, standardising variable names, parsing timestamps with their local time zone (Europe/Athens), and reshaping the data to one row per trap and collection. For each trap and calendar day of the study we also computed local sunrise and sunset times with the `getSunlightTimes` function of the `suncalc` R package[51]; these are used to summarise the weather over biologically relevant portions of the day.

Weather data

We considered three sources of weather data. The first is the ERA5-Land hourly reanalysis from the Copernicus Climate Change Service (ERA5-Land hourly), a global land-surface reanalysis at 9,km resolution that combines the land-surface model of the European Centre for Medium-Range Weather Forecasts with atmospheric forcing from the ERA5 reanalysis[52,53]. The second is daily weather-station data for Athens distributed through the Hellenic Data Service (Helix-daily). The third is 30-minute readings from temperature and relative-humidity data loggers (HOBO, Onset Computer Corporation) installed near four of the traps (BG 2, BG 3, BG 4 and BG 5; hereafter *HOBO-30min*). The ERA5-Land hourly data provide complete coverage of the three weather variables required in the MWI calculation (temperature, relative humidity and wind speed) over the entire study period at hourly resolution. The Helix-daily data also include all of the required variables and span the study period, but with daily resolution. The HOBO-30min data have the finest temporal resolution (30 min.), but they do not record wind speed and they cover only four of the six traps. We also note that the HOBO-30min relative humidity readings are systematically lower than those calculated from the ERA5-Land hourly data (Supplementary Table S3).

From the ERA5-Land hourly product we obtained 2 m dewpoint temperature, 2 m air temperature, the 10 m eastward and northward wind components, surface pressure and total precipitation. Air and dewpoint temperatures were converted to degrees Celsius, and relative humidity was derived from the dewpoint and air temperatures using the Magnus approximation, which is valid over the temperature range encountered here. Wind speed was obtained from the two wind components as $\sqrt{u_{10}^2 + v_{10}^2}$,

where u_{10} and v_{10} are the eastward and northward 10 m wind components, respectively. From these hourly variables we computed the MWI and its components at the hourly scale (see below) and only then aggregated it to daily summaries. In addition to whole-day (24 h) daily means, maxima and minima, we computed the same summaries over two biologically motivated windows: daylight hours (DT), and the two hours following sunrise together with the two hours preceding sunset (a window we refer to as AT).

Mosquito Weather Index (MWI)

The mosquito weather index (MWI), also known as the mosquito activity index, was developed within the successful cooperation of the Benaki Phytopathological Institute (Greece) and the National Observatory of Athens (Greece). The cooperation was implemented in the framework of the LIFE CONOPS project (LIFE12 ENV/GR/000466), which was funded by the European Commission in the framework of the programme LIFE + Environment Policy and Governance (2013–2018). MWI classifies mosquito activity in five classes ranging from "no activity" to "very high activity" (see Supplementary Table S1), and it has been incorporated into the Greek weather forecasting platform (https://meteo.gr). Since June 2014, an add-in has also been included in the LIFE CONOPS website, offering a link to the LIFE CONOPS mosquito weather forecast.

MWI is defined as the product of three weather-response functions—one each for temperature (F_T), relative humidity (F_H) and wind speed (F_W), each of which returns a value in $[0,1]$:

$$\mathrm{MWI} = F_T(T) \times F_H(H) \times F_W(W), \tag{1}$$

Writing T for air temperature in degrees Celsius, H for relative humidity in percent, and W for wind speed in $\mathrm{km\,h^{-1}}$, the three functions are

$$F_T(T) = \begin{cases} 0 & T \le 15, \\ 0.2T - 3 & 15 < T \le 20, \\ 1 & 20 < T \le 25, \\ -0.2T + 6 & 25 < T \le 30, \\ 0 & T > 30, \end{cases} \tag{2}$$

$$F_H(H) = \begin{cases} 0 & H < 40, \\ \dfrac{H}{55} - \dfrac{40}{55} & 40 \le H \le 95, \\ 0 & H > 95, \end{cases} \qquad F_W(W) = \begin{cases} 1 & W \le 6 \times 3.6, \\ 0 & W > 6 \times 3.6. \end{cases} \tag{3}$$

This set of equations produces an index that is zero at temperatures of 15°C and below, that rises linearly from zero at 15°C to one at 20°C, is maximal between 20 and 25°C, and declines linearly back to zero at 30°C; the humidity response is zero outside the 40–95% band and increases linearly within it; and the wind response acts as a cut-off that sets the index to zero once wind speed exceeds $6 \times 3.6 = 21.6\ \mathrm{km\,h^{-1}}$. On this basis the continuous index is mapped to five ordered activity categories, ranging from "no activity" to "very high activity", for communication to the public and to mosquito-control stakeholders (see Supplementary Table S1). The breakpoints were set from thermo-biological considerations and they are broadly consistent with field estimates of host-seeking activity in *Ae. albopictus*, which place biting between roughly 16 and 37°C with a peak near 26°C[54].

We also analyze a modified version of MWI, in which we include only the humidity and temperature functions (F_H and F_T), leaving out wind speed. We label this version FHFT and define it as:

$$\mathrm{FHFT} = F_H(H) \times F_T(T). \tag{4}$$

We compare the coefficient on FHFT and MWI across a set of models in Supplementary Figure S6.

Statistical analysis

To align the weather and trap data, daily MWI, as well as daily weather variable summaries used in comparison models, were aggregated over each trapping period: for every trap and period we took the mean of each daily weather quantity over the days the trap was active (also recording, for completeness and robustness checks, the period maximum, minimum and sum). Models

use the trapping-period *mean* of the daily summaries—for example, the primary weather covariate is the period mean of the daily-maximum MWI—with trapping effort included separately as a control rather than folded into a sum.

We fitted a total of 324 count models formed by crossing four sets of choices: (i) three outcomes—female *Ae. albopictus*, female *Cx. pipiens*, and the combined total; (ii) eighteen weather specifications; (iii) the presence or absence of a seasonal term; and (iv) three observation models. The eighteen weather specifications combine three functional forms (the single MWI value; the three raw weather variables entered linearly; and second-degree orthogonal polynomials of the three raw variables) with two daily aggregation statistics (mean and maximum) and three daily windows (24 h, DT and AT).

For an observation i (a single trap and trapping period) let Y_i denote the count of one of the three outcomes, and let $j[i]$ index the trap. All models use a log link for the conditional mean,

$$\log \mu_i = \alpha + b_{j[i]} + \beta_E \,\mathrm{effort}_i + f(\mathbf{x}_i), \qquad b_j \sim \mathcal{N}(0, \sigma^2_{\mathrm{trap}}), \tag{5}$$

where effort_i is the trapping period, $b_{j[i]}$ is a trap-level random intercept and $f(\mathbf{x}_i)$ is the weather term. The weather term takes one of three forms,

$$f_{\mathrm{MWI}}(i) = \beta_1 \,\mathrm{MWI}_i, \tag{6}$$

$$f_{\mathrm{HTW}}(i) = \beta_H H_i + \beta_T T_i + \beta_W W_i, \tag{7}$$

$$\begin{aligned} f_{\mathrm{HTW2}}(i) = {} & \beta_{H1} P_1^H(H_i) + \beta_{H2} P_2^H(H_i) \\ & + \beta_{T1} P_1^T(T_i) + \beta_{T2} P_2^T(T_i) \\ & + \beta_{W1} P_1^W(W_i) + \beta_{W2} P_2^W(W_i), \end{aligned} \tag{8}$$

where H_i, T_i and W_i are the period-summarised relative humidity, temperature and wind speed, and P_1^v and P_2^v are the linear and quadratic terms of an orthogonal polynomial basis constructed separately for each variable $v \in \{H, T, W\}$. Seasonal variants add a second-degree orthogonal polynomial in day of year,

$$f_{\mathrm{season}}(i) = \gamma_1 Q_1(d_i) + \gamma_2 Q_2(d_i), \tag{9}$$

with d_i the day of year of the collection date, so that seasonal models use $f(\mathbf{x}_i) + f_{\mathrm{season}}(i)$.

Each specification was fitted with three observation models. The Poisson model takes $Y_i \sim \mathrm{Poisson}(\mu_i)$; the negative binomial model takes $Y_i \sim \mathrm{NB}(\mu_i, \phi)$ with $\mathrm{Var}(Y_i) = \mu_i + \mu_i^2/\phi$; and the zero-inflated negative binomial (ZINB) model mixes the negative binomial with a point mass at zero,

$$\Pr(Y_i = y) = \begin{cases} \pi_i + (1-\pi_i)\,\mathrm{NB}(0 \mid \mu_i, \phi), & y = 0, \\ (1-\pi_i)\,\mathrm{NB}(y \mid \mu_i, \phi), & y > 0, \end{cases} \tag{10}$$

where $\mathrm{NB}(y \mid \mu, \phi)$ is the negative binomial probability mass function. The zero-inflation probability is modelled on the logit scale using the same weather term, $\mathrm{logit}(\pi_i) = \alpha_{\mathrm{zi}} + f(\mathbf{x}_i)$.

Models were estimated in a Bayesian framework with the `brms` package[55], using four Markov chains of 2,000 iterations each and a target average acceptance probability of 0.98. Convergence was assessed for every fitted model by computing split-$\hat{R}$ and bulk effective sample size for all parameters. Across the 216 index models underlying the results reported here, the largest $\hat{R}$ was 1.018 and the smallest bulk effective sample size 465; among the negative binomial and zero-inflated negative binomial models alone the largest $\hat{R}$ was 1.010. For the primary specification and for the models compared in Supplementary Table S5, every $\hat{R}$ was at most 1.008 and every bulk effective sample size exceeded 750. Convergence was poor in one corner of the wider grid that we do not report on: in twelve zero-inflated negative binomial models of *Ae. albopictus* combining a seasonal term with the raw weather variables, and in one negative binomial model of *Cx. pipiens* with polynomial weather terms, the zero-inflation or dispersion component is weakly identified and $\hat{R}$ reaches 3.0. Those specifications should not be interpreted, and none of the results presented here depends on them. Unless otherwise noted, the results in the main text use a single primary specification chosen a priori: a ZINB model of the trapping-period mean of the daily-maximum MWI, without a seasonal term. Trapping effort entered as a linear control; sensitivity analyses that instead used log trapping effort as a covariate or as an offset produced practically identical results (Supplementary Table S7). The remaining specifications are used to assess the robustness of the primary results across the full model grid.

The seasonal term in these models is the second-degree polynomial in day of year defined above. For the leave-future-out forecasting comparison, however—where each model is trained only on the data preceding the forecast month and must extrapolate the seasonal pattern forward—we replace this polynomial with a periodic cyclic spline in day of year. A polynomial fit to a partial year extrapolates poorly beyond the observed range and would unfairly weaken the seasonal baseline, whereas the cyclic spline is periodic (so that day 365 joins smoothly to day 1) and therefore extends across the turn of the year sensibly, giving MWI a fair seasonal competitor in the forecasting comparison.

Software and AI assistance

All data processing, modelling and figures were produced in R with the `brms`[55], `loo`, `targets` and `tidyverse` packages. During analysis and manuscript preparation, the authors used an AI coding assistant (GitHub Copilot, based on a large language model) to help develop and debug analysis code, run cross-validation comparisons, and draft and edit portions of the text, tables and figure captions. All AI-assisted code and text were reviewed, verified and edited by the authors, who take full responsibility for the accuracy and integrity of the data, analyses, results and conclusions. No AI tool is an author, and no generative-AI-created images were used.

Data availability

The BG trap and HOBO-30min data used in this study are available as a FAIR and open Frictionless Data Package at https://doi.org/10.5281/zenodo.21195178. The ERA5-Land hourly data are available from the Copernicus Climate Change Service at https://doi.org/10.24381/cds.e2161bac. The Helix-daily data are daily observations from the Athens station distributed by the Hellenic Data Service (dataset `66e1c19a-7b0e-456f-b465-b301a1130e3f`); that service was not accessible at the time of publication, and the file used here is included in the replication package at https://github.com/E4Warning/evaluating-mwi/blob/88784b4e0d/data/raw/weather_helix/athens.csv.

Code availability

The R code needed to reproduce all of the analysis and visualisations in this study is available at https://github.com/E4Warning/evaluating-mwi. We have also released an R package for calculating MWI at https://github.com/E4Warning/mwi, permanently archived on Zenodo at https://doi.org/10.5281/zenodo.22101143.

References

1. Caldwell, J. M. *et al.* Climate predicts geographic and temporal variation in mosquito-borne disease dynamics on two continents. *Nat. communications* **12**, 1233 (2021).
2. Papa, A. *et al.* Genetic characterization of west nile virus lineage 2, greece, 2010. *Emerg. Infect. Dis.* **17**, 920 (2011).
3. Danis, K. *et al.* Outbreak of west nile virus infection in greece, 2010. *Emerg. Infect. Dis.* **17**, 1868 (2011).
4. Haussig, J. M. *et al.* Early start of the west nile fever transmission season 2018 in europe. *Eurosurveillance* **23**, 1800428 (2018).
5. Pervanidou, D. *et al.* West nile virus in humans, greece, 2018: The largest seasonal number of cases, 9years after its emergence in the country. *Eurosurveillance* **25**, 1900543 (2020).
6. Carrasco, L., Utrilla, M. J., Fuentes-Romero, B., Fernandez-Novo, A. & Martin-Maldonado, B. West nile virus: An update focusing on southern europe. *Microorg. 2024, Vol. 12, Page 2623* **12**, 2623 (2024).
7. Hellenic Statistical Authority. Census results of population and housing ELSTAT 2021 (2023). Authority, H. S. (2023). Census Results of population and housing ELSTAT 2021.
8. Paz, S. Climate change impacts on west nile virus transmission in a global context. *Philos. Transactions Royal Soc. B: Biol. Sci.* **370**, 1–11 (2015).
9. Patsoula, E. *et al.* Molecular and morphological characterization of aedes albopictus in northwestern greece and differentiation from aedes cretinus and aedes aegypti. *J. Med. Entomol.* **43**, 40–54 (2006).
10. Stefopoulou, A. *et al.* Reducing aedes albopictus breeding sites through education: A study in urban area. *PLOS ONE* **13**, e0202451 (2018).
11. Bellini, R. *et al.* Practical management plan for invasive mosquito species in europe: I. asian tiger mosquito (aedes albopictus). *Travel. Medicine Infect. Dis.* **35**, 101691 (2020).
12. Badieritakis *et al.* Aedes albopictus (skuse, 1895) (diptera: Culicidae) in greece: 13 years of living with the asian tiger mosquito. *Parasitol. Res.* **117**, 453–460 (2018).
13. Patsoula, E. *et al.* Records of aedes albopictus (skuse, 1894) (diptera; culicidae) and culex tritaeniorhynchus (diptera; culicidae) expansion in areas in mainland greece and islands. *https://home.liebertpub.com/vbz* **17**, 217–223 (2017).
14. Eritja, R., Palmer, J. R., Roiz, D., Sanpera-Calbet, I. & Bartumeus, F. Direct evidence of adult aedes albopictus dispersal by car. *Sci. reports* **7**, 14399 (2017).

15. Pardo-Araujo, M., Kotov, E., Alonso, D. & Bartumeus, F. Understanding mosquito vector invasion pathways: Synergistic effects of human mobility, climate and natural dispersal. *Ecol. Lett.* **29**, e70317 (2026).

16. Lührsen, D. S. *et al.* Adult aedes albopictus in winter: implications for mosquito surveillance in southern europe. *The Lancet Planet. Heal.* **7**, e729–e731 (2023).

17. Lowe, R. & Codeço, C. T. Harmonizing multisource data to inform vector-borne disease risk management strategies. *Annu. Rev. Entomol.* **70**, 337–358 (2025).

18. Tiffin, H. S. *et al.* The influence of new surveillance data on predictive species distribution modeling of aedes aegypti and aedes albopictus in the united states. *Insects 2019, Vol. 10, Page 400* **10**, 400 (2019).

19. Kraemer, M. U. *et al.* Past and future spread of the arbovirus vectors aedes aegypti and aedes albopictus. *Nat. Microbiol. 2019 4:5* **4**, 854–863 (2019).

20. Pasquali, S. *et al.* Development and calibration of a model for the potential establishment and impact of aedes albopictus in europe. *Acta Trop.* **202**, 105228 (2020).

21. Torina, A. *et al.* Modelling time-series aedes albopictus abundance as a forecasting tool in urban environments. *Ecol. Indic.* **150**, 110232 (2023).

22. World Health Organization. Global vector control response 2017-2030. World Health Organization, Geneva (2017).

23. González-Pérez, M. I. *et al.* Unravelling the activity rhythms of urban vector mosquitoes with smart-trap technology. *Sci. Reports* **16**, 9075 (2026).

24. Balatsos, G. *et al.* Overwintering west nile virus in active culex pipiens mosquito populations in greece. *Parasites & Vectors* **17**, 286 (2024).

25. Panagopoulou, A. *et al.* Molecular detection of usutu virus in pools of culex pipiens mosquitoes in greece. *Acta Trop.* **258**, 107330 (2024).

26. European Centre for Disease Prevention and Control. Weekly updates: Seasonal surveillance in humans in 2026 for West Nile virus. https://www.ecdc.europa.eu/en/west-nile-fever/surveillance-and-disease-data/disease-data-ecdc (2026). Accessed 2026-07-26; page last updated 24 July 2026.

27. Zinszer, K. *et al.* A scoping review of malaria forecasting: past work and future directions. *BMJ open* **2**, e001992 (2012).

28. European Centre for Disease Prevention and Control. Public health guidance for assessing and mitigating the risk of locally-acquired aedes-borne viral diseases in the eu/eea. ECDC, Stockholm (2025).

29. Ogden, N. *et al.* Weather-based forecasting of mosquito-borne disease outbreaks in canada. *Can. Commun. Dis. Rep.* **45**, 127 (2019).

30. Ventura, P. C. *et al.* Forecasting the relative abundance of aedes vector populations to enhance situational awareness for mosquito control operations. *PLoS neglected tropical diseases* **18**, e0012671 (2024).

31. Erraguntla, M. *et al.* Predictive model for microclimatic temperature and its use in mosquito population modeling. *Sci. Reports* **11**, 18909 (2021).

32. McDevitt-Galles, T. *et al.* Partly cloudy with a chance of mosquitoes: Developing a flexible approach to forecasting mosquito populations. *Ecosphere* **15**, e70074 (2024).

33. Roiz, D. *et al.* Integrated aedes management for the control of aedes-borne diseases. *PLoS neglected tropical diseases* **12**, e0006845 (2018).

34. Bellver-Arnau, J., Blanco-Sierra, L., Escartín, S., Mariani, S. & Bartumeus, F. Climate-responsive vector control strategies for *aedes albopictus*. *Parasites & Vectors* **18**, 168 (2025).

35. Stiles, P. C. *et al.* Three-year assessment of integrated vector management in attica, greece: results from surveillance and control activities. *Commun. Biol.* **8**, 1533 (2025).

36. Kolimenakis, A. *et al.* Exploring public preferences, priorities, and policy perspectives for controlling invasive mosquito species in greece. *Trop. Medicine Infect. Dis.* **4**, 83 (2019).

37. Stefopoulou, A. *et al.* Reducing aedes albopictus breeding sites through education: A study in urban area. *PloS one* **13**, e0202451 (2018).

38. Kolimenakis, A. *et al.* The role of urbanisation in the spread of aedes mosquitoes and the diseases they transmit—a systematic review. *PLOS Neglected Trop. Dis.* **15**, e0009631 (2021).

39. Manica, M. *Spatio-Temporal distribution of mosquito species Aedes albopictus: the associated health risk and an assessment of the effectiveness of control interventions in Italy*. Ph.D. thesis, Università degli Studi di Roma "La Sapienza" (2018).

40. Wimberly, M. C. *et al.* Land cover affects microclimate and temperature suitability for arbovirus transmission in an urban landscape. *PLOS Neglected Trop. Dis.* **14**, e0008614 (2020).

41. Lambrechts, L. *et al.* Impact of daily temperature fluctuations on dengue virus transmission by aedes aegypti. *Proc. Natl. Acad. Sci. United States Am.* **108**, 7460–7465 (2011).

42. Brady, O. J. *et al.* Global temperature constraints on aedes aegypti and ae. albopictus persistence and competence for dengue virus transmission. *Parasites Vectors* **7**, 1–17 (2014).

43. Osman, M. *et al.* The subseasonal applications for agriculture and environment (sage) project within the world weather research programme: Making subseasonal predictions more useful for sectoral applications. *Clim. Serv.* **43**, 100693 (2026).

44. IDAlert. EpiOutlook: A platform for climate-sensitive infectious diseases. https://idalertproject.eu/epioutlook (2024). Published 11 December 2024, updated 23 April 2026; accessed 31 July 2026.

45. Palmer, J. R. *et al.* Citizen science provides a reliable and scalable tool to track disease-carrying mosquitoes. *Nat. Commun.* **8**, 1–13 (2017).

46. Bartumeus, F., Oltra, A. & Palmer, J. R. Citizen science: a gateway for innovation in disease-carrying mosquito management? *Trends parasitology* **34**, 727–729 (2018).

47. Padilla-Pozo, Á. *et al.* Assessing and correcting neighborhood socioeconomic spatial sampling biases in citizen science mosquito data collection. *Sci. Reports* **14**, 22462 (2024).

48. European Centre for Disease Prevention and Control. Guidelines for the surveillance of native mosquitoes in europe. ECDC, Stockholm (2014).

49. Darsie, R. F. & Samanidou-Voyadjoglou, A. Keys for the identification of the mosquitoes of Greece. *J. Am. Mosquito Control. Assoc.* **13**, 247–254 (1997).

50. Samanidou-Voyadjoglou, A. & Harbach, R. E. Keys to the adult female mosquitoes (Culicidae) of Greece. *Eur. Mosquito Bull.* **10**, 13–20 (2001).

51. Thieurmel, B. & Elmarhraoui, A. *suncalc: Compute Sun Position, Sunlight Phases, Moon Position and Lunar Phase* (2022). R package version 0.5.1.

52. Muñoz-Sabater, J. *et al.* Era5-land: A state-of-the-art global reanalysis dataset for land applications. *Earth system science data* **13**, 4349–4383 (2021).

53. Muñoz Sabater, J. ERA5-Land hourly data from 1950 to present (2019). Accessed 13 February 2025.

54. Yin, Q. *et al.* A field-based modeling study on ecological characterization of hourly host-seeking behavior and its associated climatic variables in Aedes albopictus. *Parasites & Vectors* **12**, 474 (2019).

55. Bürkner, P.-C. brms: An R package for Bayesian multilevel models using Stan. *J. Stat. Softw.* **80**, 1–28 (2017).

Acknowledgements

This study was supported by multiple European Union, national and international funding programmes. The work was funded under the LIFE+ Environment Policy and Governance programme through the project LIFE CONOPS (LIFE12 ENV/GR/000466) (https://www.conops.gr), as well as under the European Union's Horizon Europe programme through the projects IDAlert (Grant Agreement No. 101057554; https://idalertproject.eu), part of the EU Climate Change and Health Cluster (https://climate-health.eu), and E4Warning: Eco-Epidemiological Intelligence for early Warning and response to mosquito-borne disease risk in endemic and emergence settings (Grant Agreement No. 101086640; https://www.e4warning.eu). Additional support was provided by a) the research project entitled "Monitoring program for the presence and seasonal dynamics of mosquitoes (Culicidae) in the broader area of Moschato-Tavros, Attica" funded by the Municipality of Moschato-Tavros and b) the European Centre for Disease Prevention and Control (ECDC) under Framework Contract ECDC/2016/034, "AedesRisk project: Development of a tool to support the decision-making process for surveillance and vector control of dengue, chikungunya and Zika virus infection in Europe," specifically Work Package 3 on validation and evaluation of the model and tool, which included the field study protocol proposal for the Municipality of Moschato-Tavros (Greece) with the assistance of David Roiz, Institut de Recherche pour le Développement (IRD). This project was coordinated by Bertrand Sudre and Olivier Briët and Cedric Marsboom managed this project on behalf of the contractor, Avia-GIS. Additional support was also provided by the Green Fund project ENACT (https://enact-climate.gr/),

funded under the programme “Natural Environment and Innovative Actions 2023”. The funders had no role in study design, data collection and analysis, decision to publish, or preparation of the manuscript.

We are grateful to Evangelia Zavitsanou for her valuable support in creating the map used in this article.

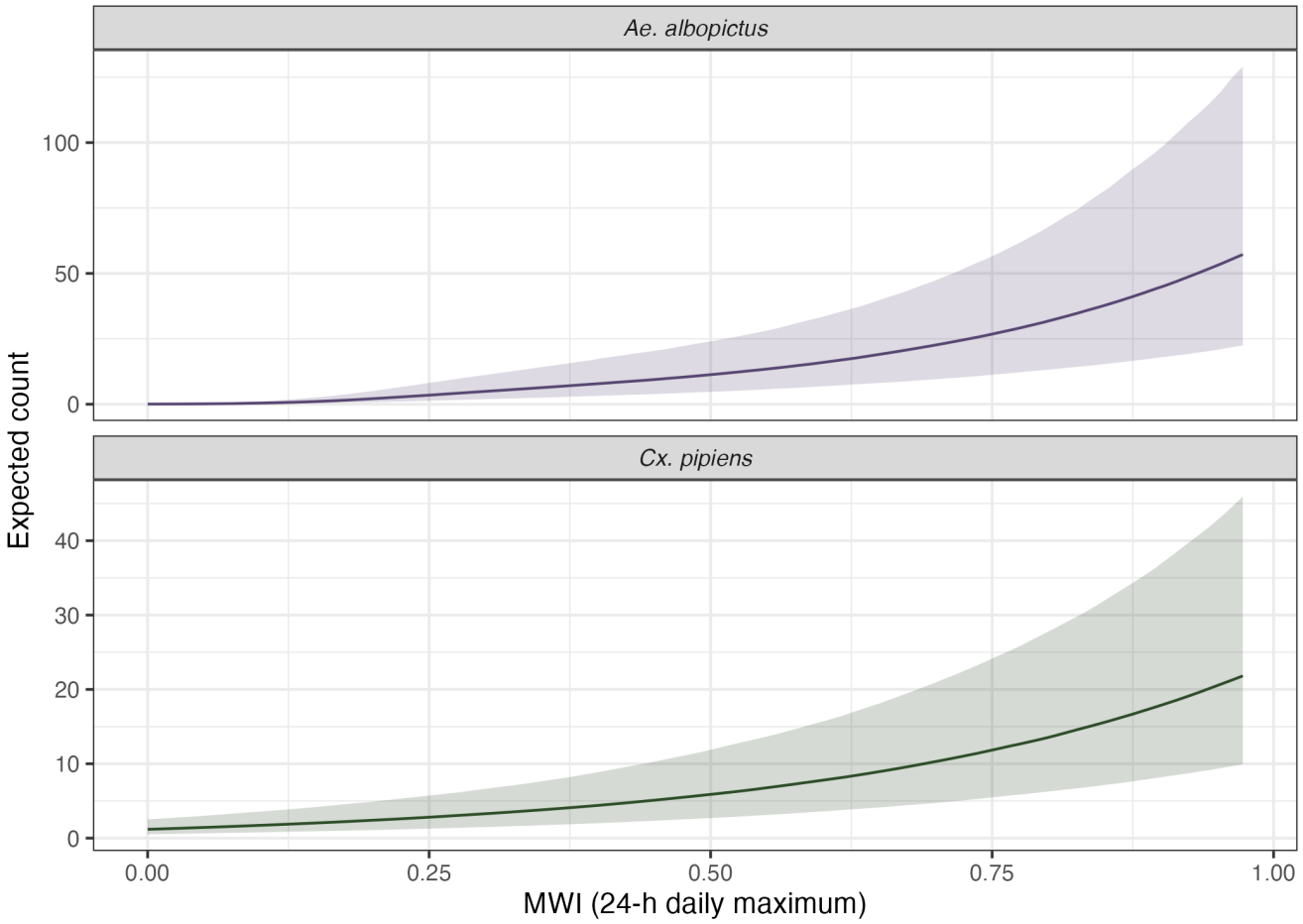
Author contributions statement

A.M. conceived the study, A.M., G.B., V.K., and D.P. carried out the field work, and J.P. conducted the statistical analysis, produced the figures and software, and curated the data. A.M., G.B. and J.P. drafted the manuscript, and R.L., F.B., K.L., C.G., I.L., V.K., and D.P. critically revised it, adding intellectual content. All authors reviewed the manuscript.

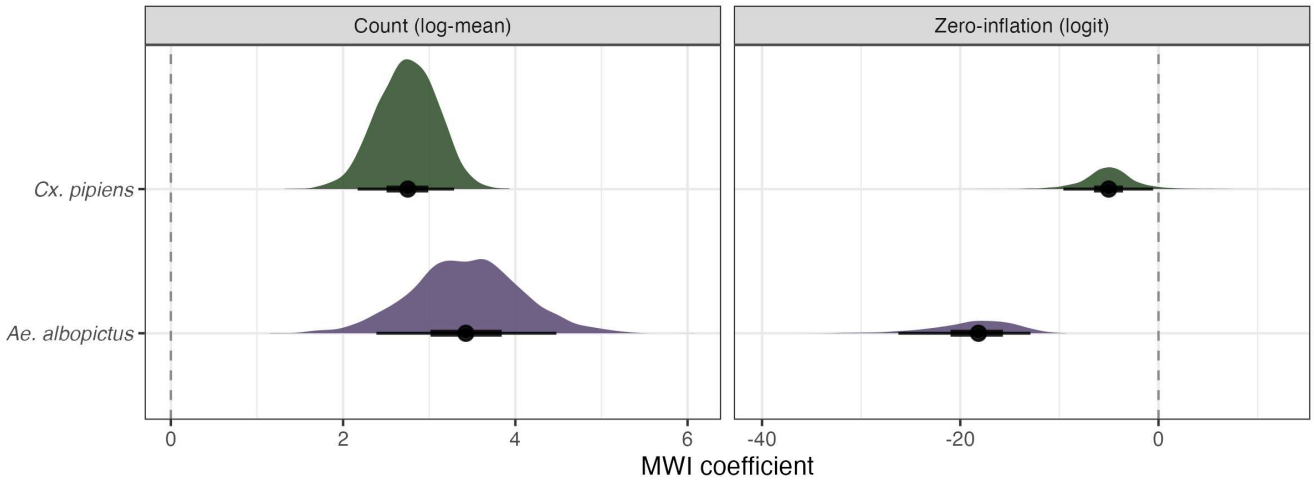
Additional information

Competing interests

The authors declare no competing interests.



(a)



(b)

Figure 1. Relationship between MWI and BG trap counts in the primary zero-inflated negative binomial models (24-hour daily-maximum MWI). (**a**) Expected trap count as a function of MWI for *Ae. albopictus* (top) and *Cx. pipiens* (bottom); curves are posterior medians and shaded bands 90% credible intervals, with trapping effort held at its mean and trap random intercepts ignored (note the independent count axes). (**b**) Posterior distributions of the MWI coefficient for both species: the left group shows the count-component coefficient (log-mean scale) and the right the zero-inflation-component coefficient (logit scale); points are posterior medians with 50% and 90% credible intervals (thick and thin bars) and the dashed vertical line marks zero.

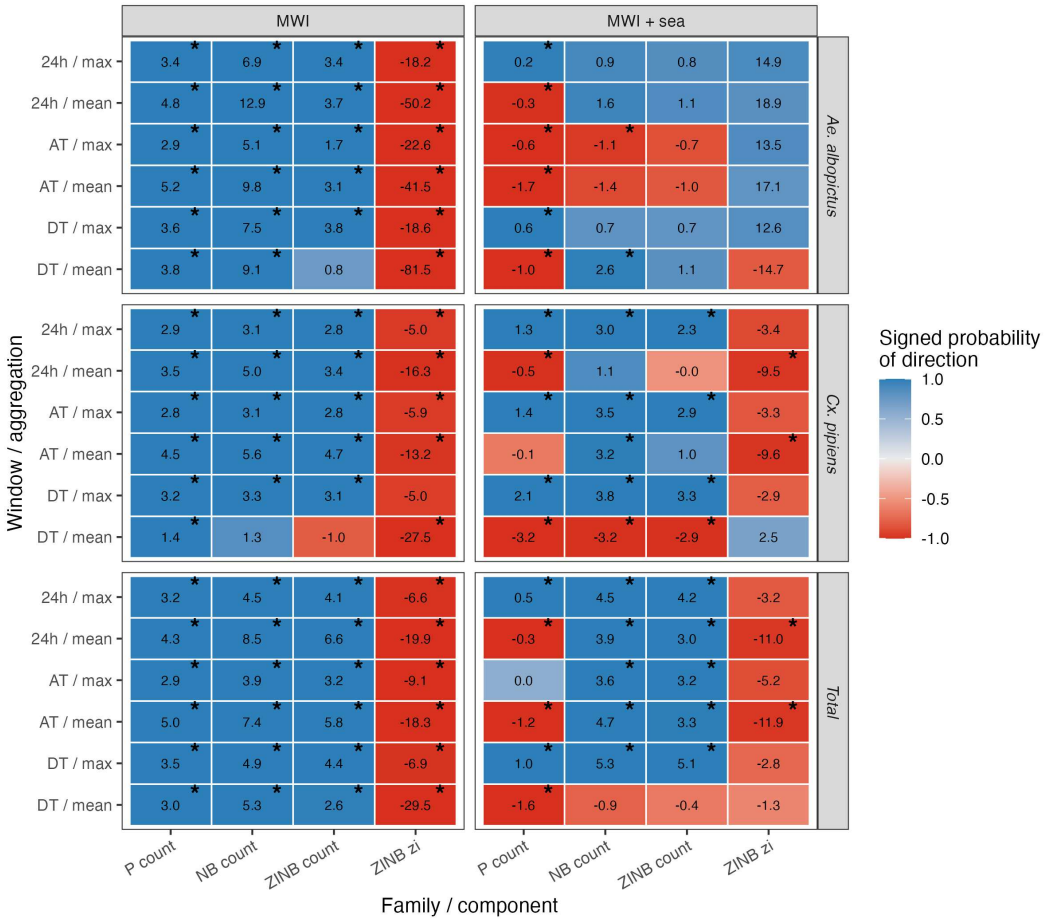


Figure 2. MWI coefficient across the set of models. Cell fill is coloured based on the signed probability of direction (blue positive, red negative; colour saturation reflects certainty), and an asterisk marks cells whose 90% credible interval excludes zero. The value labels show the posterior median coefficient on the model's native link scale (log for the count component, logit for the zero-inflation component). Each row shows a different combination of daily aggregation window—full 24 hour vs. two-hours right after sunrise and two-hours right before sunset (AT) vs. full daylight hours (DT)—and aggregation statistic—maximum vs. mean. Columns show model distribution family and component, split by whether or not a seasonality term is included; facet rows are species—*Ae. albopictus*, *Cx. pipiens*, and both species pooled. A grid with additional model specifications is given in Supplementary Figure S6.

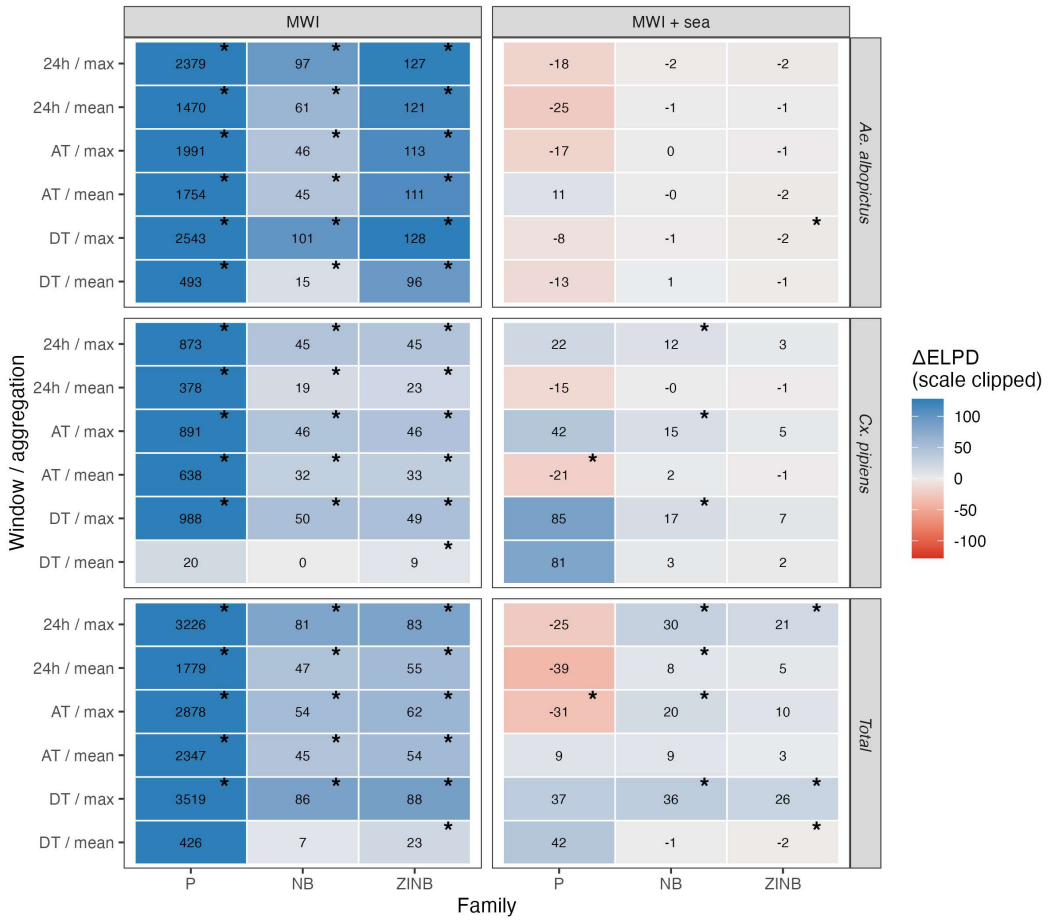


Figure 3. Leave-one-out predictive gain (ΔELPD) of each MWI model relative to its matched no-MWI version, across a set of model specifications. Blue indicates MWI improves held-out prediction and red indicates it worsens it; asterisks mark cells whose 90% intervals (ΔELPD $\pm 1.645 \cdot$SE) exclude zero. Because the Poisson models produce artificially large values—reflecting how poorly a Poisson comparator fits these overdispersed counts, rather than any extra information in MWI—the fill scale is clipped to the non-Poisson range (Poisson cells are shown at the extreme colour); cell labels show the actual ΔELPD values. Within a given species, family and seasonality all six MWI variants are compared against the same no-MWI model, so differences between those cells are equal to differences between the MWI models themselves and can be read directly; ΔELPD is not comparable across families or across species, since it is a log density under a particular likelihood and response. Rows are aggregation window—24 hour, daylight hours (DT), or 2 hours after sunrise and before sunset (AT)—and aggregation statistic (mean or max); columns are model distribution family (Poisson, negative binomial, or zero-inflated negative binomial); facet rows are species and facet columns are MWI with and without a seasonality term. A grid showing comparisons across additional model specifications is given in the Supplementary Figure S7.

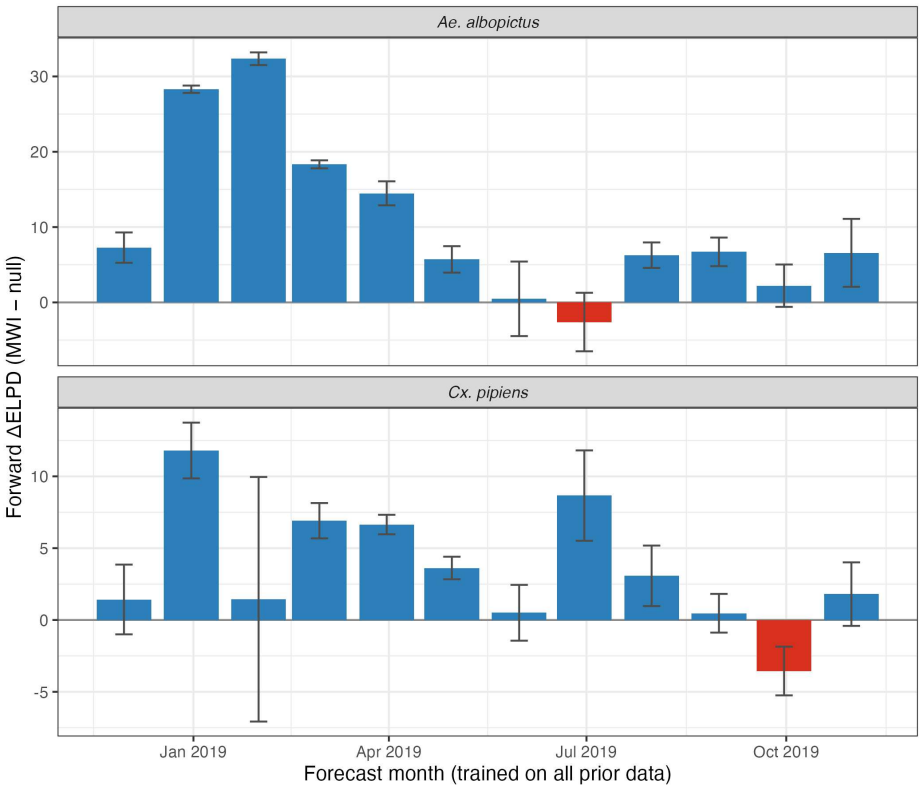


Figure 4. Monthly leave-future-out forecast skill against a *non-seasonal* baseline: forward ΔELPD (MWI added to a model with only trapping effort and trap random effects, minus that null model), refitting on past data only and forecasting the next month with observed weather. Positive bars are months where MWI improves the forecast; error bars are ±1 SE.

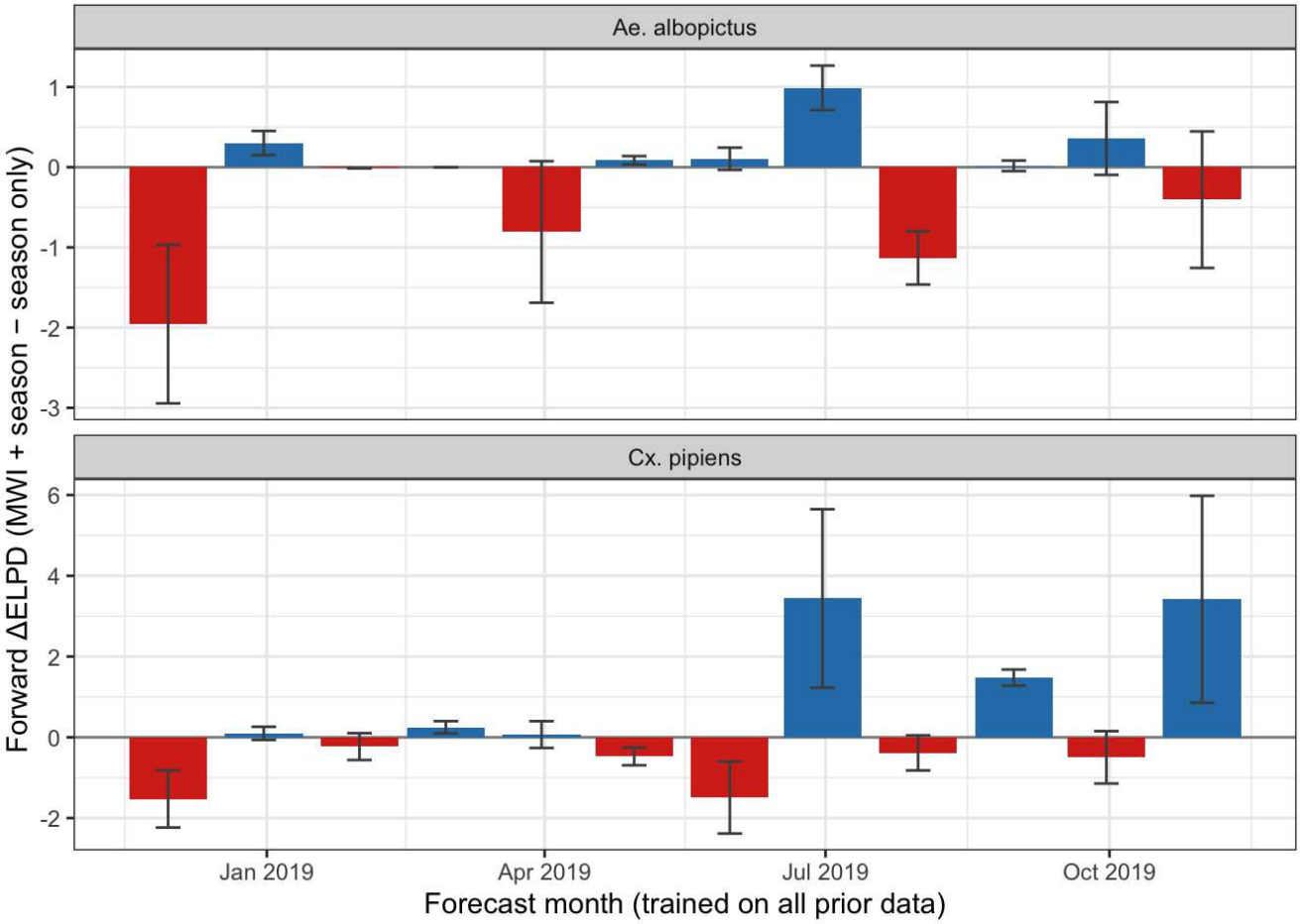


Figure 5. Monthly leave-future-out forecast skill: forward ΔELPD (MWI plus a cyclic seasonal trend minus the seasonal trend alone), refitting on past data only and forecasting the next month with observed weather. Positive bars are months where MWI improves the forecast; error bars are ±1 SE.



Figure 6. Locations of the six BG-Sentinel traps within the municipality of Moschato-Tavros, Attica, Greece, shown over satellite imagery. Map created with ArcGIS Pro (3.0.0), available from Esri (Marathon Data, GR).

Supplementary Files

This is a list of supplementary files associated with this preprint. Click to download.

- evaluatingmwioverleafsupplementalinfo.pdf